Magnetotransport properties of $Hg_{1-x}Re_xBa_2Ca_2Cu_3O_{8+\delta}$ superconductors

J. Roa-Rojas
Departamento de Física, Universidad Nacional de Colombia, A.A. 14490, Bogotá, D.C., Colombia

M.T.D. Orlando
Departamento de Física, Universidade Federal do Espírito Santo, 29060-900, Vitoria ES, Brasil

E. Baggio-Saitovich
Centro Brasileiro de Pesquisas Físicas, Rua Xavier Sigaud 150, 22290-180, Rio de Janeiro RJ, Brazil

P. Pureur
Instituto de Física, Universidade Federal do Rio Grande do Sul, 91501-970, Porto Alegre RS, Brazil

Recibido el 23 de julio de 2001; aceptado el 22 de enero de 2002

Systematic measurements on Hall and longitudinal resistivities as a function of temperature in $Hg_{1-x}Re_xBa_2Ca_2Cu_3O_{8+\delta}$ *(x=0.18)* ceramic samples were effectuated. These measurements were performed in magnetic fields *H=0, 10, 20, 40* and *50 kOe*, applied perpendicularly to the transport current orientation. In the normal phase, the Hall coefficient is positive and may be accurately fitted to $R_H = 1/aT + b$. The Hall angle varies approximately as predicted by Anderson's formula. When the temperature approaches from above the mean-field critical temperature T_c, the Hall resistivity decreases abruptly as a consequence of thermal fluctuations. Below T_c and for $H = 10$and *20 kOe*, the Hall response changes signal, going passing through a minimum and becoming positive again before the zero resistance state is obtained. For stronger applied fields, the Hall resistivity remains positive in the mixed phase, though its qualitative shape, preserving the local minimum below T_c. We ascribe the double sign reversal feature to combined effects of thermal fluctuations and vortex motion. Close to the zero resistance state, the Hall resistivity varies as a power law of the longitudinal resistivity, with a field-independent exponent. This result may be interpreted as evidence of a vortex-glass transition.

Keywords: Superconductivity; Transport Properties; Mixed State.

Reportamos mediciones de las resistividades longitudinal y Hall en función de la temperatura para muestras cerámicas de $Hg_{1-x}Re_xBa_2Ca_2Cu_3O_{8+\delta}$ *(x=0.18)*. Tales mediciones se efectuaron en presencia de campos magnéticos *H=0, 10, 20, 40* y *50 kOe*, aplicados en dirección perpendicular a la orientación de la corriente de transporte. En la fase normal, el coeficiente Hall es positivo y se ajusta a la relación $R_H = 1/aT + b$. El ángulo de Hall varía aproximadamente conforme lo predice la fórmula de Anderson. Por encima y muy próximo de la temperatura crítica de campo medio T_c, la resistividad Hall disminuye abruptamente a causa de las fluctuaciones térmicas. Por debajo de T_c, para $H = 10$ y *20 kOe*, la respuesta Hall cambia de signo, pasa a través de un mínimo local y vuelve a ser positivo antes de alcanzarse el estado de resistencia nula. En campos mayores, la resistividad Hall permanece siempre positiva en el estado mixto pero conserva su forma, presentando un mínimo local por debajo de T_c. Nosotros atribuimos el doble cambio de signo a efectos combinados de fluctuaciones térmicas y movimiento de vórtices. Cerca del estado de resistencia cero, la resistividad Hall varía como una ley de potencias de la resistividad longitudinal con un exponente independiente del valor del campo magnético. Este resultado es interpretado como evidencia de una transición de tipo vidrio de vórtices.

Descriptores: Superconductividad; propiedades de transporte; estado mixto.

PACS: 74.25.Fy; 74.60.Ec; 74.40.+k

1. Introduction

$HgBa_2Ca_{n-1}Cu_nO_{2n+2+\delta}$ superconductors have been extensively studied since their discovery [1]. The most interesting compound of the series is the $n = 3$ member, *Hg-1223*, which shows the highest critical temperature ($T_c \approx$ *135 K*) [2]. Measurements of magnetotransport properties in this system reveal a great similarity with the *Tl*-based cuprate [3]. The Hall effect, which hasn't been intensively studied in these high-T_c superconductors, exhibits unusual features: in the normal phase the Hall coefficient R_H, is proportional to $1/T$, contrasting the expectations for nonmagnetic metals [4]. Consequently, the Hall angle presents a quadratic temperature dependence. Proposes based on the Luttinger liquid model provide a natural explanation for anomalous features of transport data in several high-T_c superconductors [5]. Within this picture, spin charge separation in the CuO_2 planes results in two different rates: a longitudinal (transport relaxation rate $1/\tau \sim T$) and a transverse (Hall relaxation rate $1/\tau_H \sim T^2$ with a temperature-independent term added to both rates when impurity scattering is present). The first gives the well-known linear-T resistivity, while the second gives the Hall dependence $\cot\theta_H^N \propto AT^2$. In the mixed

phase, the Hall resistivity often shows striking changes of sign which have been attributed to anomalous vortex motion [6], superconducting fluctuations [7] or to a difference between charge densities in the core and far outside the vortices [8]. Furthermore, powerlaw dependence between the Hall and longitudinal resistivities, $\rho_{xy} = A\rho_{xx}^{\beta}$, have been found in the regime approaching the zero resistance state of several HTSC samples [9].

The synthesis of the unsubstituted compound poses serious problems at pressures ¡ *50 bar* due mainly to HgO_δ instability [10]. This is the reason why most authors have studied the doping of high-valence cations in $Hg_{1-x}M_xBa_2Ca_2Cu_3O_{8+\delta}$, where *M=Pb, Bi, W* or *Re* [11-13]. In this communication we report longitudinal and Hall resistivities measurements (as a function of the temperature in magnetic fields up to *50 kOe*) in polycrystalline samples of $Hg_{1-x}Re_xBa_2Ca_2Cu_3O_{8+\delta}$,denoted *Hg(Re)-1223*, where $x = 0.18$. The normal and superconducting states are qualitatively discussed and the phenomenological parameters are also determined.

2. Experimental

Hg(Re)-1223 polycrystalline samples were prepared by the vacuum quartz tube technique. $Ba_2Ca_2Cu_3O_x$ (99.9%, PRAXAIR) and ReO_2 (99.9% Aldrich) powders were combined in a 1:0.18 molar ratio and homogenized in an agate mortar. A rectangular pellet was axially compacted under 0.5 GPa and annealed at 850°C in oxygen flow for 15 h. The pellet was subsequently homogenized, compacted and annealed again at 930 ˚C in oxygen flow for 15 h. This two-step process intends to assure both homogeneity of rhenium and elimination of carbonates in the samples. HgO (99% Aldrich) and the precursor were mixed in a nominal stoichiometric quantity prior to palletizing. Other precautions, such as the use of a dry box, were not taken in contrast with other authors [14]. The heating and cooling rates were 120 ˚C/h and the holding time at maximum temperature in all thermal cycles was fixed to 5 h. The length of the quartz capsule was 80 mm with 8.0 mm of inner diameter and 2.0 mm of wall thickness. A Thermobaryc Analysis (TBA) by means of a pressure sensor was developed (together with the measured temperature) by using the well-known decomposition reaction of HgO_δ; the estimated experimental accuracy is ± 0.2 bar. The TBA sensor was calibrated with a standard manometer for every new measurement to obtain the calibration line. The samples were grounded in agate mortar and dried in an oven under N_2-atmosphere for 1 h. Finally, the resulting powder was sieved below 65 μm. The aim of this process was to dissagglomerate the powder so that intergranular currents remain close to a minimum [15]. Then, this powder was pressed in 1 cm diameter pallets. The existence of 1223 structural phase was observed in X-ray diffraction patterns [15].

Four silver paste contacts were implanted to perform the resistivity measurements. These contacts were obtained by using a lowfrequencylowcurrent AC technique between the zero-resistance state and room temperature. Special care was taken in the temperature interval close to the transition in order to determine accurately the fluctuation contribute to conductivity. Magnetic fields of *0, 10, 20, 40* and *50 kOe* were applied parallel to the current direction. Studies of the fluctuation magnetoconductivity were carried when the field was applied in accordance with the Field Cooling procedure. Temperature was measured with a Pt sensor (*500* Ω at $300K$) corrected for magnetoresistivity effects. The technique permits to measure temperatures with a resolution better than $2m$K. A large number of resistivity *vs.* T points were recorded while the temperature was continuously increased or decreased across the transition in rates not exceeding $3\ K/h$. Using a numerical method we accurately determined the temperature derivative of the resistivity, $d\rho/dT$, at temperatures near the transition. Two additional silver paste contacts were implanted on the sample to measure the Hall voltage. The Hall and longitudinal voltages were measured simultaneously using the same lowfrequency AC technique and a Stanford SR530 lockin amplifier as a null detector. Another lock-in amplifier and an inductive bridge Dekatran model 73 were implement to compensate the possible longitudinal contributions to the Hall voltage. The Hall resistivity ρ_{xy} was calculated by the relation $\rho_{xy} = d/iV_H$, where d is the thickness of sample, i represents the transport current and V_H is the Hall voltage.

3. Longitudinal and Hall resistivities

3.1. Longitudinal resistivity ρ_{xx}(T,H)

At high temperatures (*180 K <T<260 K*) resistivity shows a linear dependence with temperature, as shown in Fig. 1. This behavior is described by

$$\rho_{xx}^R = \rho_o + \frac{d\rho_{xx}^R}{dT}T, \tag{1}$$

where $d\rho_{xx}^R/dT = 0,07414(m\Omega.cm/K)$ and $\rho_0 = 3,86194(m\Omega.cm)$. Above and closer to the superconducting transition temperature, the longitudinal resistivity exhibits a pronounced rounding (for *T < 240 K*), which is attributed to strong effects of thermal fluctuations [16]. The critical temperature, determined at the maximum of temperature derivative of resistivity, is $T_c = 133.1K$ in absence of magnetic field. When magnetic field is applied, effects of vortex-dynamics due to Lorentz-force action are observed, which affect the temperature transition and expand the limit of the so-called zero-resistance state, denoted by $T_{c0}(H)$, in direction to lower temperatures region [17]. In high temperatures, *T > 180 K*, it is observed that the longitudinal resistivity $\rho_{xx}(T)$ has an approximately linear temperature dependence when compared with non-doped *Hg-1223* samples, as reported by other authors [16].

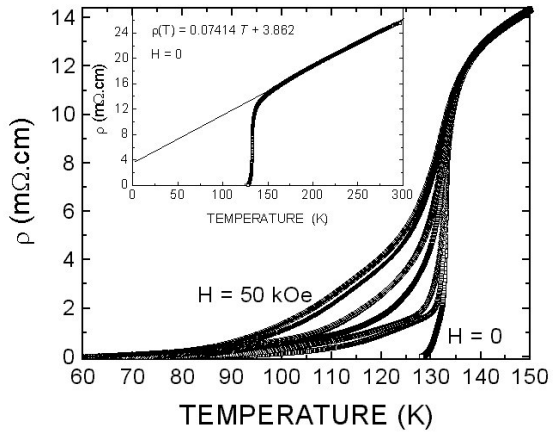

FIGURE 1. Resistivity transition of a Hg(Re)-1223 bulk sample for several external fields applied perpendicularly to the current orientation. The applied magnetic fields are *H = 0, 0.5, 2.5, 10, 20, 40* and *50 kOe*. The inset exemplifies the normal feature of resistivity as a function of temperature according with equation (1)

3.2. Hall resistivity ρ_{xy}(T,H) in the normal state

As expected, the Hall resistivity is positive for $T > T_c$ and exhibits a linear dependence with the applied magnetic field. The normal Hall resistivity varies inversely with temperature and fits the expression $\rho_{xy}^N(T,H) = \mu_0 H/0,0084\ T + 0,05$, for the temperature interval *170 K* $< T <$ *260 K* and H measured in *kOe*, as shown in Fig. 2. Thus, the carrier density of transport current is given by $n_H^N = 0,62\,T + 3,61$, in conformity with Fig. 3. This result is in accordance with reports for Tl- and Bi-based families of cuprate materials [4]. It is important to elucidate that the mechanisms of charge transport in high temperature superconductors do not have the same characteristics as those of metals or semiconductor materials. Hence, this carrier density cannot be extracted simply even in the context of Boltzmann theory as the cases of isotropic scattering, parabolic bands and circular Fermi surface [18].

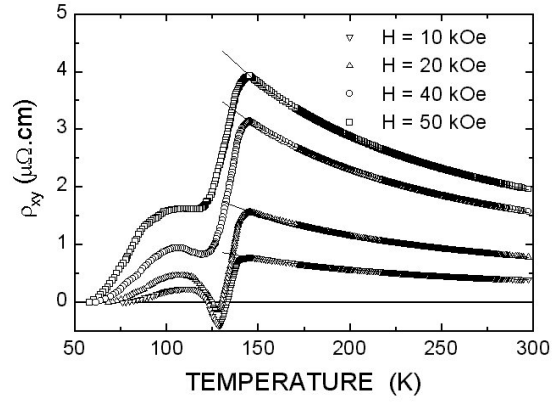

FIGURE 2. Hall characteristic in both normal and superconducting states as measured in a Hg(Re)-1223 polycrystalline sample. Magnetic fields *H = 10, 20, 40* and *50 kOe* were applied.

The Hall angle in the normal state, θ_H^N, was obtained from the approximation given by $\cot\theta_H^N = \rho_{xx}^N/\rho_{xy}^N$. The experimental result is shown in Fig. 4, where it is easy to see that the cotangent of the Hall angle satisfies the Anderson's formula $\cot\theta_H^N = AT^2 + C(x)$, with A the doping grade and $C(x)$ the magnetic impurities concentration [5].

The fit to Anderson's formula in the temperature interval between $170K$ and $260K$ is given by $\cot\theta_H^N = 7.02\ T^2 + 4337/\mu_0 H$, where H is expressed in *kOe*. Most authors interpret this behavior introducing the concept of elemental excitation (quasi-particle) from the t-J model [19]. These quasiparticles, so-called *spinons*, generate the scattering responsible by this dependence. In the transition approach the Hall response presents a reversal of slope. Below and very close to T_c the Hall resistivity exhibits a change of sign, with a minimum and annuls close to temperature value $T_{c0}(H)$. This behavior, which is shown in Fig. 2, occurs in the regime dominated by fluctuations in the phase of the order parameter of Ginzburg-Landau, as observed in bulk samples of $RBa_2Cu_3O_{7-\delta}$ [17].

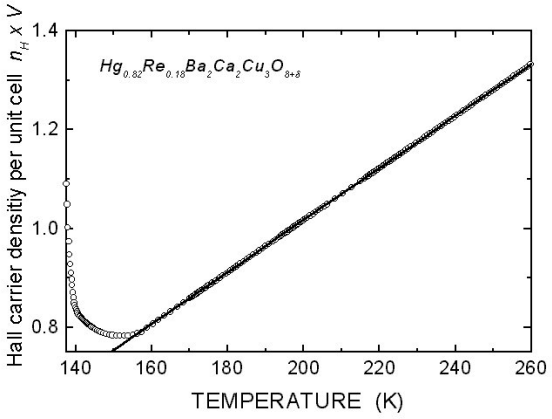

FIGURE 3. Carrier density related to the current transport in the *Hg(Re)-1223* sample.

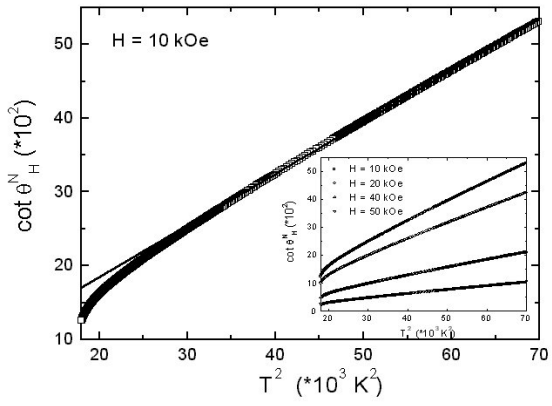

FIGURE 4. Quadratic temperature dependence of Hall angle in applied magnetic field *H = 10 kOe*. At high temperatures the fit to the Anderson's formula is observed. The inset shows the characteristic behavior for several magnetic fields *H=10, 20 40* and *50 kOe*.

3.3. Hall resistivity ρ_{xy}(T,H) in the superconducting state

Below bulk critical temperature, Hall resistivity experiments exhibit two sign changes on applied magnetic fields *H ≤ 20 kOe*, as shown in Fig. 5. For magnetic fields *H > 20 kOe* the Hall response is positive but the observed tendency in low fields is preserved. This result is compatible with identical reports for *$HgBa_2CaCu_2O_{6+\delta}$* thin films [20].

In order to investigate the role of thermal superconducting fluctuations we plot in Fig. 5(a) the quantity [21]

$$\chi_\sigma = -\frac{d}{dT}\ell n\,\Delta\sigma, \tag{2}$$

where $\Delta\sigma$ is the fluctuation longitudinal conductivity or conductivity excess [21], for the same temperatures and fields. This is obtained by subtracting the regular conductivity σ_R form the measured conductivity $\sigma = 1/\rho$; *i.e.* $\Delta\sigma = \sigma - \sigma_R$. First term is determined by extrapolating the normal resistivity, as observed in the inset of Fig. 1. The quantity χ_σ has been used to discern the various fluctuation regimes contributing to the conductivity of the HTSC, including the critical 3DXY one [21], indeed, if $\Delta\sigma \cong (T - T_c)^{-\lambda}$ then χ_σ^{-1} may be fit to a straight line whose intersection with the T axis and slope allows to determine the critical temperature T_c of the fluctuation regime and the corresponding critical exponent λ, respectively.

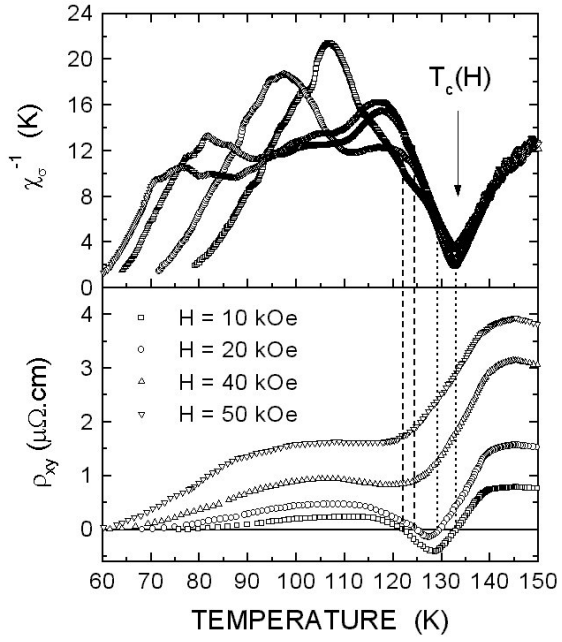

FIGURE 5. Comparative results between: (a) the quantity χ_σ^{-1}, defined in Eq. (2), near the pairing critical temperature and in the mixed phase. The $T_c(H)$ specified in the picture corresponds to the maximum of the numerical temperature derivative of longitudinal resistivity. (b) Hall resitivity of Hg(Re)-1223 in the same temperature interval. Measurements are performed in the quoted fields.

Previous studies in granular HTSC samples [22] have shown that the V-shaped sharp minimum in χ_σ^{-1}, observed in Fig. 5(a), is practically coincident with the pairing T_c. The almost field independent and linearly T-dependent behavior around this position identifies the region where the magnetotransport properties are strongly dominated by thermal fluctuations. Comparing Figs. 5(a) and (b) we note that the first sign inversion in the Hall resistivity occurs inside this temperature region. Thus, a negative Hall contribution due to fluctuations is likely to produce the signal change close to T_c.

At lower temperatures vortices become stable entities and the Hall effect resulting from their motion should be considered. As this contribute is expected to be of the same sign as the Hall effect in the normal phase [23], a second sign reversal in the total Hall resistivity might occur in systems having weak pinning, which is the case of the strongly anisotropic *Hg(Re)1223*.

In the regime approaching the zero resistance state, the Hall and longitudinal resistivities scale as $\rho_{xy} = A\rho_{xx}^{\beta}$ with $\beta = 1.5 \pm 0.2$. This behavior, shown in Fig. 6, is interpreted either as evidence of vortex motion in the presence of pinning [24] or as a vortex glass effect [9]. We mention, however, that contrasting with observations in $HgBa_2CaCu_2O_{6+\delta}$ films [24], the β exponent is independent of the field in the studied range of temperatures for our *Hg(Re)1223* samples.

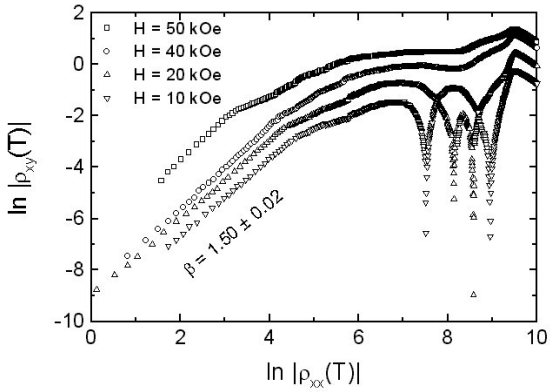

FIGURE 6. Scaling of Hall resistivity in the zero resistance state approach for a Hg(Re)-1223 sample with several applied magnetic fields.

4. Conclusions

Normal- and superconducting-states measurements of longitudinal and Hall resistivities were performed on polycrystalline *Hg(Re)-1223* samples. It is observed that the longitudinal resistivity both in normal and superconducting phases, is essentially similar to high-T_c ceramics of *YBaCuO* and *BiSrCaCuO* [25-26]. The Hall response for $T > T_c$ is strongly temperature dependent, up to high temperatures, for the motion of the charge carriers in the *CuO_2* planes. Two changes of the Hall signal are observed in the superconducting transition. We suggest as the possible cause of the neg-

ative contribution to Hall response, which manifests the first reversal Hall resistivity combined effects of thermal fluctuations and skew scattering of quasiparticles by screening current loops [27]. The second change of the Hall signal can be related to the strong anisotropic nature of these high-T_c systems. The relevance of the strong vortex dynamics in these disordered systems is clearly evident in the scaling of $\rho_{xy} \sim \rho_{xx}^{\beta}$ near the characteristic temperature of the zero resistance state.

Acknowledgments

We are indebted to Dr. R. Hurtado for carefully reading this manuscript. This work is partially funded by the Brazilian Ministry of Science and Technology under contract No. PRONEX/FINEP/CNPq 41.96.0907.00. The Brazilian agencies CAPES and CNPq and the Colombian agency COLCIENCIAS also gave partial support.

1. S.N. Putilin, E.V. Antipov, O. Chmaissen, M. Marezio, *Nature* **362** (1993) 226
2. O. Chmaissen, Q. Huang, E.V. Antipov, S.N. Putilin, M. Marezio, S.M. Loureiro, J.J. Capponi, J.L. Tholence, A. Santoro, *Physica C* **217** (1993) 265
3. J.R. Thompson, J.G. Ossandon, D.K. Christen, B.C. Chakoumakos, Yang Ren Sun, M. Paranthaman, J. Brynestad, *Phys. Rev. B* **48** (1993) 14031
4. N.P. Ong, in: *Physical Properties of High Temperature Superconductors*, vol. II, ed. D.M. Ginsberg (World Scientific, Singapore, 1990) p. 459
5. P.W. Anderson, *Phys. Rev. Lett.* **67** (1991) 2092
6. Z.D. Wang, J. Dong and C.S. Ting, *Phys. Rev. Lett.* **72** (1994) 3875
7. W. Liu, T.W. Clinton, A.W. Smith and C.J. Lobb, *Phys. Rev. B* **55** (1997) 11802
8. M.V. Feigel'man, V.B. Geshkenbein, A.I. Larkin and V.M. Vinokur, *JETP Lett.* **62** (1995) 835
9. J. Luo, T.P. Orlando, J.M. Graybeal, X.D. Wu and R. Muenchausen, *Phys. Rev. Lett.* **68** (1992) 690
10. S.M. Loureiro, C. Stott, L. Philip, M.F. Gorius, *et al*, *Physica C* **272** (1996) 94
11. S. Hahakura, J. Shimoyama, O. Shiino, T. Hasegawa, K. Kitazawa, K. Kishio, *Physica C* **235-240** (1994) 915
12. D. Pelloquin, A. Maignan, S. Malo, M. Hervieu, C. Michel, B. Raveau, *J. Mater. Chem.* **5** (1995) 701
13. B. Reveau, C. Michel, M. Hervieu, A. Maignan, *J. Mater. Chem.* **5** (1995) 803
14. G.B. Peackock, I. Gameson, P. Edwards, *Adv. Mater.* **9** (1997) 248
15. A. Sin, A.G. Cunha, A. Calleja, M.T.D. Orlando, E. Baggio-Saitovich, F.G. Emmerich, S. Piñol, X. Obradors, *Physica C* **306** (1998) 34; Agustin Sin, Alfredo G. Cunha, Albert Calleja, Marcos T. D. Orlando, Francisco G. Emmerich, Elisa Baggio-Saitovich, Mercé Segarra, Salvador Piñol, Xavier Obradors, *Advanced Materials* **10** (1998) 1126
16. A. Schilling, O. Jeandupeux, I.D. Guo, H.R. Ott, *Physica C* **216** (1993) 6
17. J. Roa-Rojas, D.A. Landínez T., P. Pureur, *Phys. Stat. Sol.* (b) **220** (2000) 513
18. J.M. Harris, H. Wu, N.P. Ong, R.L. Meng, C.W. Chu, *Phys. Rev. B* **50** (1994) 3246
19. T.R. Chien, Z.Z. Wang, N.P. Ong, *Phys. Rev. Lett.* **67** (1991) 2088
20. W.N. Kang, S.H. Yun, J.Z. Wu, D.H. Kim, *Phys. Rev. B* **55** (1997) 621
21. P. Pureur, R. Menegotto Costa, P. Rodrigues Jr., J. Schaf and J.V. Kunzler, *Phys. Rev. B* **47** (1993) 11420
22. J. RoaRojas, R. Menegotto Costa, P. Pureur, P. Prieto, *Phys. Rev. B* **61** (2000) 12457
23. J. Bardeen and M.J. Stephen, *Phys. Rev. A* **140** (1965) 1197
24. W.N. Kang, D.H. Kim, S.Y. Shim, J.H. Park, T.S. Hahn, S.S. Choi, W.C. Lee, J.D. Hettinger, K.E. Gray and B. Glagola, *Phys. Rev. Lett.* **76** (1996) 2993
25. R. Menegotto Costa, P. Pureur, L. Ghivelder, J.A. Campá, I. Rasines, *Phys. Rev. B* **56** (1997) 10836
26. A.R. Jurelo, J.V. Kunzler, J. Schaf, P. Pureur, J. Rosenblatt, *Phys. Rev. B* **56** (1997) 14815
27. J. Roa-Rojas, P. Pureur, M.T.D. Orlando and E. Baggio-Saitovich, *Physica C* **341-348** (2000) 1043.